

Synergy of CALIOP and ground-based solar radiometer data to study statistical characteristics of aerosols in regions with a low aerosol load [†]

Anatoli Chaikovsky^{1,*}, Andrey Bril¹, Philippe Goloub², Zhengqiang Li³, Vladislav Peshcherenkov¹ and Fiodar Asipenka¹, Luc Blarel², Gael Dubois², Mikhail Korol¹, Aliaksandr Lapionak², Aleksey Malinka¹ and Natallia Miatselskaya¹, Thierry Podvin² and Ying Zhang³

¹ Institute of Physics of the NAS of Belarus, 220072 Minsk, Belarus; anatoli.chaikovsky@gmail.com;

andrey.bril@ifanbel.bas-net.by; v.pescherenkov@ifanbel.bas-net.by; n.miatselskaya@dragon.bas-net.by;

a.malinka@ifanbel.bas-net.by; m.korol@ifanbel.bas-net.by; bazylevich-vladislav@mail.ru; f.osipenko@tut.by;

² Laboratoire d'Optique Atmosphérique, Département de Physique, Université de Lille, Villeneuve d'Ascq, France;

philippe.goloub@univ-lille.fr; thierry.podvin@univ-lille.fr; Luc.Blarel@univ-lille.fr;

gael.dubois@univ-lille.fr; aliaksandr.lapionak@univ-lille.fr

³ State Environment Protection Key Laboratory of Satellite Remote Sensing, Aerospace Information Research

Institute, Chinese Academy of Sciences, Beijing 100101, China; lizq@radi.ac.cn; zhangying02@radi.ac.cn

* Correspondence: anatoli.chaikovsky@gmail.com

[†] Presented at 5th International Electronic Conference on Remote Sensing, 07–21 November 2023; Available online:

<https://ecrs2023.sciforum.net/>.

Abstract: Statistical characteristics of combined lidar and radiometric measurements obtained from satellite lidar CALIOP and ground-based sun-radiometer stations are used as input dataset for retrieving altitude profiles of aerosol parameters (LRS-C technique). The signal-to-noise ratio of the input satellite lidar signals increases when averaging over a large array of measured data. An algorithm and a software package for processing the input dataset of the LRS-C sounding of atmospheric aerosol in the region with medium and low aerosol load have been developed. The paper presents results of studying long term changes of the aerosol mode concentration profiles in the regions of East Europe (AERONET site *Minsk*, 53.92°N, 27.60°E) and East Antarctic (AERONET site *Vechernaya Hill*, 67.66°S, 46.16°E).

Keywords: combined lidar and radiometer sounding; aerosol; CALIOP; AERONET; SONET

1. Introduction

A method of combined lidar and radiometer sounding of atmospheric aerosol with application of CALIOP [1] lidar data, measured in the area of radiometric stations (LRS-C technique) has been proposed and developed in [2–4]. In comparison with aerosol sounding by ground-based integrated lidar and radiometric stations (LRS method) [5], the application of LRS-C technique has increased the number of potential measuring sites up to 500 all over the planet, except for polar regions with a latitude greater than 80 °, which observations are not available due to the inclination of the CALIOP orbit plane, equal to 98.2°.

The LRS-C technique can be applied for studying large scale aerosol changes over the areas with ground-based sun radiometer stations supplementing or replacing the data of stationary lidar systems. However, the main advantage of the LRS-C method is that it can be applied for the comprehensive analysis of large datasets obtained from regular radiometric measurements by the AERONET [6] and SONET [7] stations, and from the CALIOP lidar sounding. The satellite lidar CALIOP was launched in June 2006.

Special algorithms and software are needed to work with large experimental datasets. Processing of LRS-C data is sequentially performed by two relatively independent procedures – collection and statistical processing of LRS-C datasets and retrieving mean values of aerosol parameters from the statistical characteristics of lidar and radiometric measured data.

The first procedure is easily performed using specialized programs. The amount of calculations at the second stage of processing is limited to a list of statistical parameters, required to characterize the process under the study, and only slightly depends on the amount of initial experimental data. So, the statistical version of the LRS-C technique is optimal for processing large radiometric and lidar datasets when a region with a large number of radiometric stations is studied.

The lidar part of the input data at the stage of solving the ill-posed inverse problem is presented by the ensemble-averaged lidar signal. The signal-to-noise ratio of the averaged lidar signals is much higher than the corresponding values for individual measurements. As a result, the statistical variant of the LRS-C technique can be used to study aerosol layers with the extremely low aerosol load, like in Antarctic and mountain regions.

2. Method and processing procedure

2.1. Idea of the method

The idea of the statistical variant of the LRS-C technique is to use statistical characteristics of lidar and radiometric sounding datasets as input information for calculating the statistical characteristics of the aerosol parameters. It was necessary to make changes to the LRS-C data processing algorithm LIRIC-2 [2], the main of which are:

- adding statistical characteristics of aerosol particles to the aerosol optical model;
- defining the equations of relation between the statistical characteristics of input datasets and the parameters of the aerosol optical model;
- correcting the algorithms for the final stage of LRS-C data processing, i.e. determination of the target parameters of the aerosol model, which minimize the differences between the measured and calculated statistical characteristics of the input datasets.

The lidar equation that determines the relationship between the lidar signal and the parameters of the aerosol optical model is a linear form applied to the aerosol optical parameters only for small values of the aerosol optical depth. Otherwise, the relation between the statistical characteristics of the lidar signal and the aerosol optical parameters should be determined taking into account the probability density function (PDF) of the corresponding optical parameters. Similarly to [8], we use the normal PDF function to characterize aerosol optical parameters.

2.2. Statistical ensemble of input data

The first step in the LRS-C data processing procedure is the collection of input statistical dataset. Certain requirements have been defined for the procedure of coordinated ground-based and satellite LRS-C measurements. For each radiometrical station, a “measuring circle” with a radius ΔR of the order of 100–200 km is defined. The section of the CALIOP trajectory with length Δl , whose projection forms the chord of the circle, is the “measuring segment”. The lidar signals registered withing this segment are summed up after the “cloud-screen” procedure and forming an element of the input array of lidar data. The multiparameter method for identifying clouds and aerosol types along the CALIOP sounding path is described in [9]. The results are presented in the “Vertical Feature Mask Product” file, which is available in [10] along with the package of lidar data.

The trajectory of the CALIPSO satellite is sun-synchronous. The sounding of the atmosphere by the CALIOP lidar in the area of the radiometric station occurs approximately at the same Coordinated Universal Time (UTC).

The array of aerosol optical parameters calculated from radiometric measurements within the time window $\Delta t = \pm 2$ hours from satellite overpass time, forms an element of the input radiometric dataset.

3. Results

3.1. Temporal aerosol changes

The statistical variant of the LRS-C technique was used to study of aerosol changes in the region of the AERONET site "Minsk", 53.920°N, 27.601°E between 2006 and 2023. The radius of measuring circle was 200 km. So, "measuring circle" covered almost the entire territory of Belarus. The sun-synchronous orbit of the CALIPSO overpasses measuring circle ("overpass event") approximately 90 times a year at 11:00 UTC.

The input statistical ensemble of lidar and sun-radiometer data includes day-time measured lidar signals at 11:00 UTC and radiometer data in the range 9:00 – 13:00 UTC.

The key stage of LRS-C data processing is the selection of an aerosol optical model whose parameters need to be retrieved. Two variants of the LRS-C data processing algorithm were tested. They differ in the initial aerosol model and sets of input data:

- the AERONET two-mode aerosol model with fine (F) and coarse (C) aerosol modes; the ensemble of input data includes arrays of lidar signals at 532 and 1064 nm and column optical parameters of aerosol modes, calculated from radiometric observations;
- the more detailed three-mode aerosol model in which the coarse mode is divided into two submodes of coarse spherical (C1) and coarse non-spherical (C2) particles; the ensemble of input data is supplemented with rows of the depolarized lidar signals at 532 nm and column values of the "sphericity" (ratio of the column concentration of C1 particles to the column concentration of total coarse particles).

The results of processing and analysis of the LRS-C data are presented in figures 1 – 3.

Fine particulate concentration profiles are almost identical for both variants for total period and for seasons, Fig. 1 and Fig. 2. The sum of (C1) and (C2) concentration profiles is close to the profile of the total concentration of coarse particles.

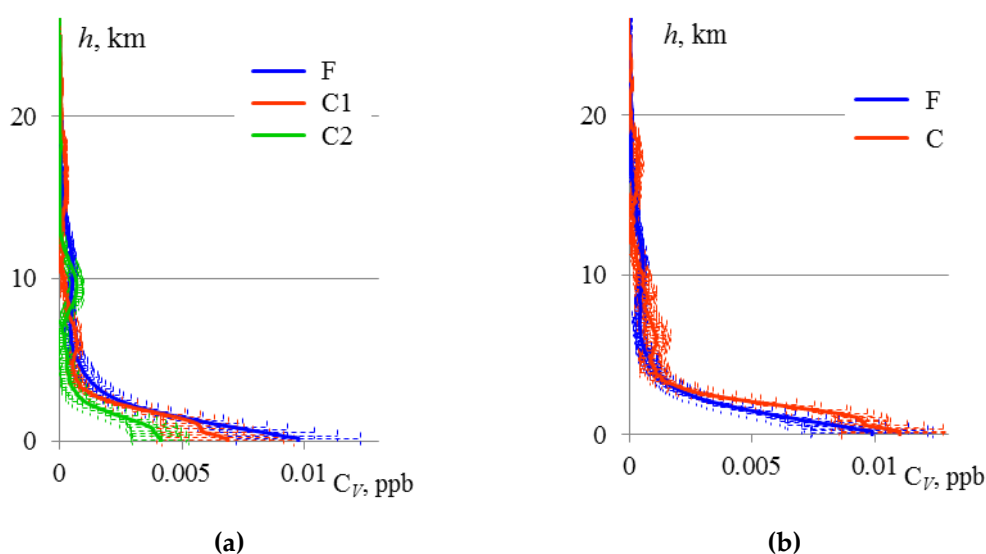


Figure 1. Altitude profiles of the aerosol average volume concentrations, C_V [cm^3/cm^3] (a) – the three-mode aerosol model, (b)- the two-mode aerosol model; horizontal bars are uncertainties of concentration; the total number of overpass events, $N = 1384$; $\text{AOD} = 0.15/0.11$ (average/standard deviation, 532 nm).

The formation of average concentration profiles shown in Fig. 1 occurs under the influence of processes, which determine the total amount of aerosols matter as a result of emissions from regional natural and anthropogenic sources and long-range transport of atmospheric impurities, as well as features of geophysical characteristics.

These factors are subject to seasonal changes. Seasonal mean concentration profiles of aerosol fractions are shown in Fig. 2. The upper boundary of the mixing layer shifts from 0.6 – 0.8 km (W) to 2 – 2.5 km (S). Concentration of non-spherical aerosol particles is weak in lower atmospheric layer during cold time of thee year.

The total LRS-C data was divided into 4 periods. Changes in the concentration profiles of aerosol fractions, their column concentrations and AOD (532) are presented in Figure 3 and Table 1. There was a trend towards decrease the total amount of small particles (fine mode) and their concentration in the lower layer.

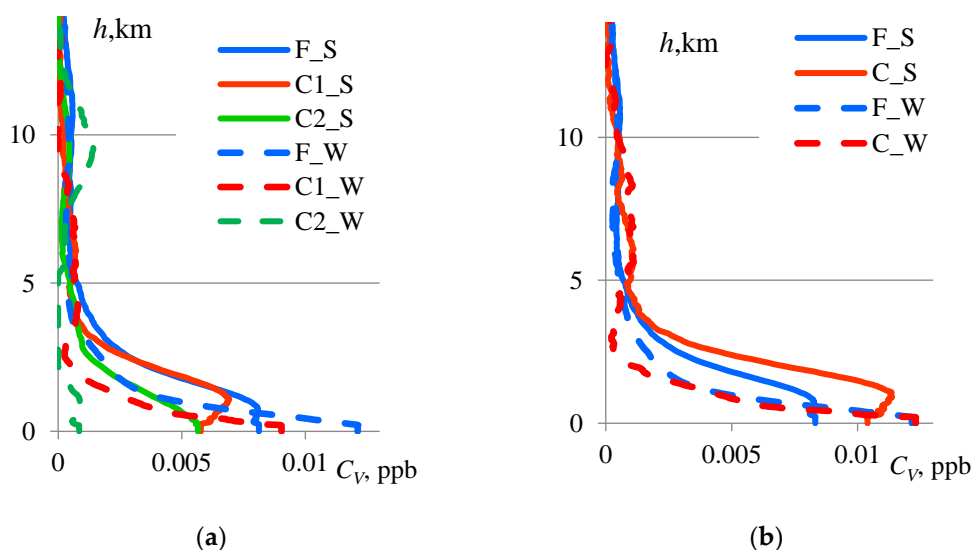


Figure 2. Seasonal changes of aerosol volume concentration profiles; similar to Fig.1; additional letters, S/W, indicate half-year seasons: S - Apr.÷Sept., N=709; AOD = 0.16/0.12; W°-°Oct.÷March; N=675; AOD (532) = 0.13/0.10.

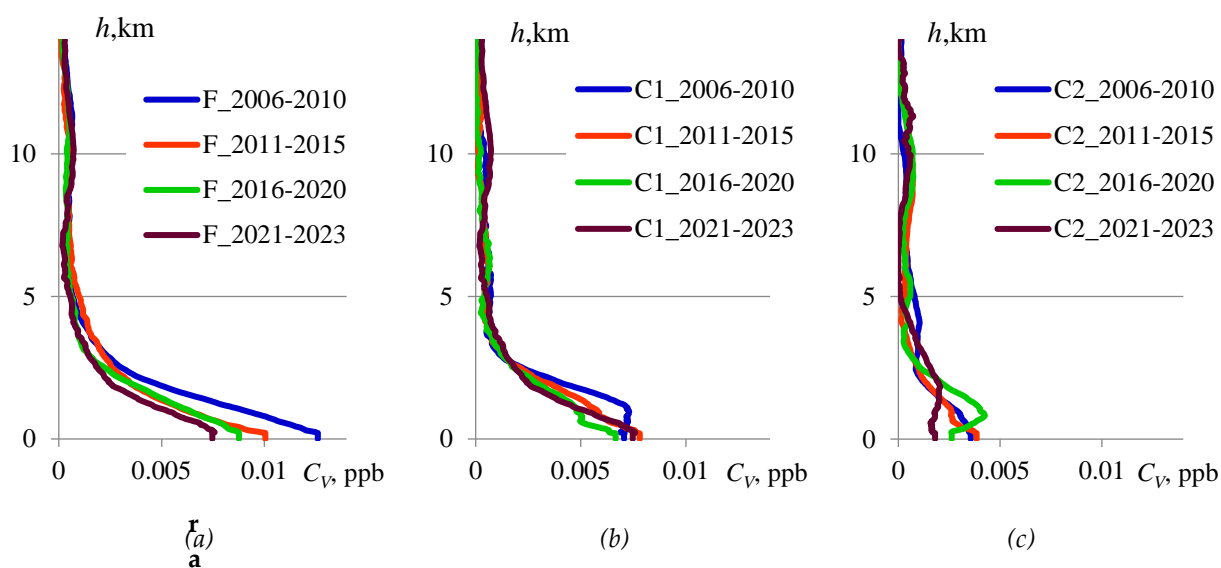


Figure 3. Temporal variations in aerosol mode volume concentration profiles; similar to Fig.1; **(a)** fine mode; **(b)** coarse spherical mode; **(c)** coarse spheroid mode. Time periods are indicated in the legends; N=379; 415; 401; 188.

Table 1. Temporal changes of column concentrations of aerosol modes and AOD (*aver./st. dev.*)

Time period	Fine (F)	Coarse Spherical (C1)	Coarse Spheroid (C2)	AOD (532)
2006 - 2010	0.029	0.022	0.011	0.19/0.15
2011 - 2015	0.023	0.019	0.011	0.15/0.11
2016 - 2020	0.021	0.018	0.012	0.14/0.10
2021 - 2023	0.019	0.019	0.010	0.12/0.08

3.2. Aerosol concentration profiles in the East Antarctic region

Results of radiometric measurements at the AERONET site *Vechernaya Hill*, 67.66°S, 46.16°E and CALIOP lidar data in this region during the Antarctic summer seasons (December - March) from 2008 to 2023 are presented in Fig.4 . Day-time CALIOP measurements were carried out in *Vechernaya Hill* about 12:00 UTC

Figure 4a shows altitude profiles of the aerosol average volume concentration for fine and coarse modes. Small particles make up the dominant aerosol fraction. The maximum concentration value is recorded in the lower layer. Course particles are often found in the middle troposphere. Their column concentration is much lower, and the variability is much higher in comparison with the parameters of fine particles.

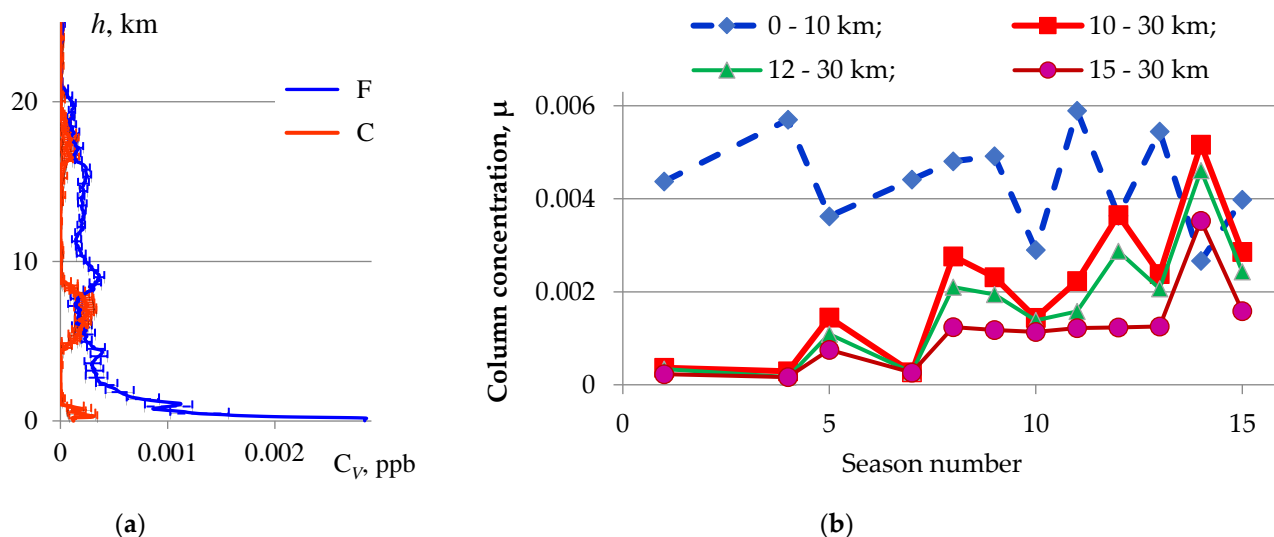


Figure 4. (a) Altitude profiles of the aerosol average volume concentrations, (F) fine mode, (C) coarse mode; N = 482; AOD= 0.045/0.017 (b) Temporal changes of column concentrations of fine aerosol mode. The boundaries of the aerosol layers are indicated in the legend of the diagram.

Figure 4b demonstrates temporal changes of total amounts of small particles in tropospheric and stratospheric aerosol layers during measuring seasons. The 1st measuring season was held in 2008 - 2009 , etc., last 15th season - in 2022-2023. The increase in the column amount of small particles in the stratosphere during the 12th measuring season (2019–2020) is probably a consequence of the rise of forest fire smoke into the stratosphere in Australia [11]. Hunga Tonga–Hunga Ha‘apai volcano eruption during December 2021 – January 2022 sent clouds of ash about 60 km height into the atmosphere and could increase the amount of matter in the stratosphere in the Antarctic area, including the *Vechernaya Hill* region.

4. Discussion and conclusions

Synergy of data from ground-based radiometric measurements and satellite lidar sensing led to new information on large-scale spatial and temporal changes of aerosol fractions.

Statistical variant of LRS-C technique and software LIRIC-2 can be used as a comprehensive tool for processing large datasets of combined ground-based radiometer observations by AERONET and SONET stations, as well as satellite lidar CALIOP sounding.

The new technique provided studying altitude distribution of average aerosol parameters in the regions with the low atmospheric aerosol load.

Author Contributions: Conceptualization, A.C., P.H. and Z.L.; methodology, A.C., A.B., P.H., Z.L., V.P., A.M. and N.M.; software, V.P., A.M., N.M., A.B. and Y.Z.; data curation, A.C., V.P., A.M., N.M., T.P., and Y.Z.; investigation, F.A., L.B., G.D., M.K., A.L. T.P. and V.P.; validation, V.P., F.A., L.B., G.D., T.P., M.K., A.L., and Y.Z.; writing-review and editing, A.C., A.B., P.H., Z.L., V.P., A.M., and N.M.; formal analysis, Y.Z., F.A., L.B., G.D., M.K., and A.L.; writing - original draft, A.C., A.M., N.M., P.H., and Z.L.; supervision, A.C., P.H., and Z.L. All authors have read and agreed to the published version of the manuscript.

Funding: This work was partly supported by the Belarusian Republican Foundation for Fundamental Research through the project F22KI-035.

Institutional Review Board Statement: Not applicable.

Informed Consent Statement: Not applicable.

Data Availability Statement: AERONET data are freely available from <https://aeronet.gsfc.nasa.gov> (accessed on 04 September 2023). CALIOP data are freely available from <https://www.opendap.org> (accessed on 04 September 2023).

Acknowledgments: The authors thank NASA CALIPSO team for the data products used in this publication. The authors thank Brent Holben, Pawan Gupta, Elena Lind, and David Giles (NASA/GSFC) for advancement and managing of the AERONET program.

Conflicts of Interest: The authors declare no conflict of interest.

References

1. The Cloud-Aerosol Lidar and Infrared Pathfinder Satellite Observation (CALIPSO). Available online: <https://www-calipso.larc.nasa.gov/> (accessed on 31 October 2023).
2. Chaikovsky, A.; Chaikovskaya, L.; Denishchik-Nelubina, N.; Fedarenka, A.; Oshchepkov, S. Lidar&radiometer inversion code (LIRIC) for synergetic processing of EARLINET, AERONET and CALIPSO lidar data. *EDJ Web of Conferences* **2018**, *176*, pp. 1-4. <https://doi.org/10.1051/epjconf/201817608007>
3. Chaikovsky, A.; Bril, A.; Fedarenka, A.; Goloub, P.; Hu, Q.; Lopatin, A.; Lapyonok, T.; Miatselskaya, N.; Torres, D.; Fuertes, D.; Peshcharenkov, V.A.; Podvin, T.; Popovich, I.; Liu, D.; Li, Z.; et al. Synergetic Observations by Ground-Based and Space Lidar Systems and Aeronet Sun-Radiometers: A Step to Advanced Regional Monitoring of Large Scale Aerosol Changes. *EPJ Web Conferences* **2020**, *237*, 1-4. <https://doi.org/10.1051/epjconf/202023702035>
4. Chaikovsky, A.P.; Bril, A.I.; Fedarenka, A.S.; Peshcharankou, V.A.; Denisov, S.V.; Dick, V.P.; Asipenka, F.P.; Miatselskaya, N.S.; et al. Synergy of ground-based and satellite optical remote measurements for studying atmospheric aerosols. *J. Appl. Spectrosc.* **2020**, *86*, 1092 – 1099.
5. Chaikovsky, A.; Dubovik, O.; Holben, B.; Bril, A.; Goloub, P.; Tanre, D.; et al. Atmos. Meas. Tech., **9** (2016) 1181–1205. Lidar-Radiometer Inversion Code (LIRIC) for the retrieval of vertical aerosol properties from combined lidar/radiometer data: development and distribution in EARLINET. *Atmos. Meas. Tech.* **2016**, *9*, 1181–1205.
6. NASA; Goddard Space Flight Center; AERONET; Aerosol Robotic Network. Available online: <https://aeronet.gsfc.nasa.gov/> (accessed on 05 September 2023).
7. Li, Z.Q.; Xu, H.; Li, K.T.; Li, D.H.; Xie, Y.S.; Li, L.; Zhang, Y.; Gu, X.F.; Zhao, W.; Tian, Q.J. Comprehensive study of optical, physical, chemical and radiative properties of total columnar atmospheric aerosols over China: An overview of Sun-sky radiometer Observation NETwork (SONET) measurements. *Bull. Am. Meteorol. Soc.* **2018**, *99*, 739–755.
8. Chaikovsky, A.P.; Bril, A.I.; Peshcharenkov, V.A.; Метельская, N.S.; Malinka, A.V.; Осипенко, F.P.; Korol, M.M.; Goloub, P.; Podvin, T.; Blarel, L.; Dubois, G.; Lapionak, A.; Z. Li, Z.; Zhang, Y. A statistical approach to the synergy of data from CALIOP and ground-based radiometric stations for studying altitude profiles of aerosol parameters. *J. Appl. Spectrosc.* (submitted).
9. Liu, Z.; Vaughan, M.A.; Winker, D.M.; Hostetler, C.H.; Poole, L.R.; Hlavka, D.; Hart, W.; and McGill, M. Use of probability distribution functions for discriminating between cloud and aerosol in lidar backscatter data. *Journal of Geophysical Research* **2004**, *109*, D15202, doi:10.1029/2004JD004732, 2004.
10. OPeNDAP [Electronic resource]: Advanced Software for Remote Data Retrieval. Mode of acc., <https://www.earlinet.org>, (accessed on 31 October 2023).
11. Gonzalez, R.; Toledano, C.; Roman, R.; et al. Characterization of Stratospheric Smoke Particles over the Antarctica by Remote Sensing Instruments. *Remote sensing* **2020**, *12*, 3769. <https://doi.org/10.3390/rs12223769>.